Int J Adv Manuf Technol (2016) 87:3315–3323
DOI 10.1007/s00170-016-8693-2

ORIGINAL ARTICLE

An experimental study of nitrogen gas influence on the 443 ferritic stainless steel joints by double-shielded welding

Yong Zheng[1] · Yichen Wang[1] · Heng Li[1] · Wenqing Xing[1] · Xinye Yu[1] · Peng Dong[1] · Wenxian Wang[1,2] · Guangwei Fan[3] · Jie Lian[3] · Min Ding[1,2]

Received: 20 January 2016 / Accepted: 27 March 2016 / Published online: 13 April 2016

Abstract This study addressed the comparison of microstructures and mechanical properties of gas tungsten arc welding (GTAW) of 443 super pure ferritic stainless steel which are protected by three different kinds of shielding gas during welding process: pure argon, argon in the inner layer combined with nitrogen in the outer layer (simple double-layer gas), and argon-5 %nitrogen in the inner layer combined with nitrogen in the outer layer (mixed double-layer gas). As a result, in the center of the welds protected by nitrogen and argon, it formed equiaxed grains which achieving the purpose of grain refinement, while there were all columnar grains in the weld protected by pure argon. The experimental results showed that the depth/width ratio of the welds shielded by simple double-layer gas had been increased. Additionally, with the addition of nitrogen in the shielding gas, the hardness and impact toughness of the weld metal and heat-affected zone (HAZ) were improved when the heat input was the same. The relationships between microstructures and mechanical properties of 443 ferritic stainless steel joints were studied by optical microscope and scanning electron microscope combined with energy-dispersive spectrometer.

✉ Min Ding
dingmin@tyut.edu.cn

[1] College of Materials Science and Engineering, Taiyuan University of Technology, 79 West Yingze Street, 030024 Taiyuan, Shanxi Province, China

[2] Key Laboratory of Interface Science and Engineering in Advanced Materials, Ministry of Education, 79 West Yingze Street, 030024 Taiyuan, Shanxi Province, China

[3] Technology Center, Taiyuan Iron and Steel (Group) Company Limited, 030003 Taiyuan, China

Keywords GTAW · Ferritic stainless steel · Nitrogen · Grains refinement

1 Introduction

In general, equiaxed crystal structures in welds are expected rather than columnar crystal structures due to its excellent mechanical properties. The welds with finer grains will exhibit higher strength and better toughness because there exist more boundaries in the equiaxed crystal structures which can prevent deformation and crack propagation when the welds are stressed to deform. Based on solidification theory, increasing cooling rate or decreasing temperature gradient can promote the columnar-to-equiaxed transition (CET). So far, many experimental or theoretical studies have been developed for CET, such as adding alloying elements [1–4], cryogenic [2, 5], magnetic field [6, 7], ultrasound [8], and vibration [8, 11]. However, the capital equipment costs of cryogenic, magnetic field, and ultrasound are high, while adding alloying elements have not been uniform. In order to overcome these limits, a new double-layer gas-shielded welding method was invented by Lu Shanpin [9]. The inner layer gas can influence the weld bead morphology and the weld shape due to Marangoni convection. The outer layer gas can be decomposed and dissolved in the molten pool, which can change the element content in the weld metal and heat-affected zone (HAZ) metal. The new double-layer gas-shielded welding method can change the microstructures and properties of weld metal and HAZ metal simultaneously.

With 21 wt% Cr, less than 0.01 wt% C, and 0.2 wt% Ti, 443 stainless steel is a new low-cost super-pure ferritic stainless steel with good machinability and corrosion resistance, which made 443 stainless steel more attractive in pipe and automobile exhaust funnel. But, its poor notch impact

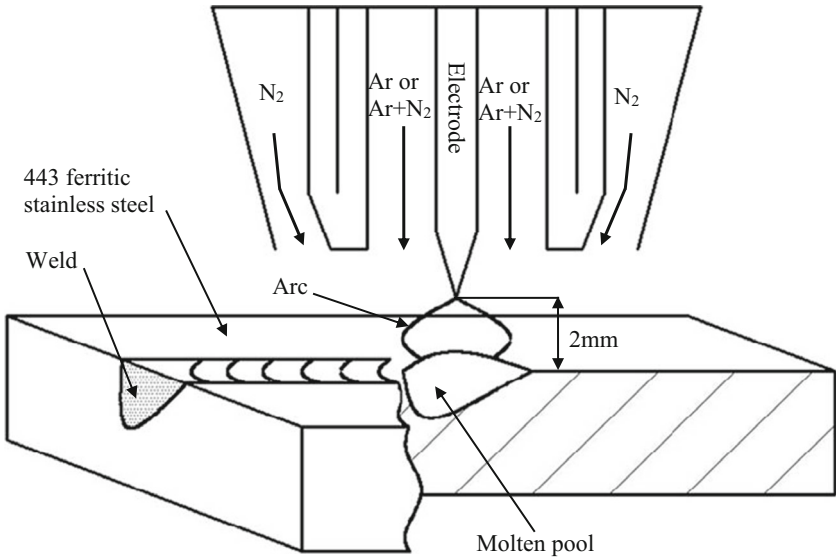

Fig. 1 Schematic diagram of GTAW torch with a gas hood during the welding process

toughness of the weld metal and HAZ metal caused by coarse crystal structures and grain growth in HAZ greatly limits its application. As mentioned above, people took a lot of methods to refine the grain size of welds in ferrite stainless steel. However, many factors limit the development of above methods. Many researchers have studied the influence of shielding gas compositions. Nitrogen (N) is a strong γ stabilizer, which can improve the strength of welding joints [13–14]. In addition, N may assist in initiating the homogenization of the Cr or Ti distribution in these two phases [2, 10, 11, 12–17]. N atoms produce a distorted lattice of Fe matrix which results in an increase in the hardness and strength of the steel [18]. Paulraj Sathiya and M. Y. Abdul Jaleel have reported that nitrogen-shielded weld metal microstructure had finer grains and fewer amounts of equiaxed grains [19]. Appropriate control over these factors can result in a significant improvement in the CET, hardness, and toughness of the joints and, in particular, its toughness of fusion zone. Given the above considerations, a mixed gas of Ar and N_2 as shielding gas has recently been used to absorb the nitrogen into the WM of the DSSs [13–14]. N element can be decomposed and dissolve in the molten pool and diffuse into the HAZ when the HAZ is at high temperature [12, 14]. The double-layer gas-shielded welding method with gas nitriding is a potential method of welding 443 stainless steel to improve the toughness of the weld metal and HAZ metal, simultaneously.

However, it is very rare to view literatures about adding nitrogen into molten pool during the welding of ferritic stainless steel. In this paper, the welds protected by different contents of N_2 in Ar and pure Ar during the process of welding 443 ferritic stainless steel were studied. Effects of nitrogen on the formation of equiaxed grains in the center of the welds were investigated. The relationships between the microstructures and mechanical properties of the joints were analyzed.

Table 1 Welding parameters

Welding conditions	Welding current (A)	Welding speed (cm/min)	Electrode gap (mm)	Shielding gas
1	80	100	2	Ar
2	80	100	2	Ar inner + N_2 outer
3	100	100	2	Ar inner + N_2 outer
4	80	100	2	Ar-5 %N_2 inner + N_2 outer

2 Experimental procedures

In this study, various shielding gases were used in the welding process, pure Ar, simple double-layer gas, and mixed double-layer gas, to explore the effect of nitrogen on the welding of 443 ferritic stainless steel. In order to achieve the purpose of double-layer gas-shielded welding method, a gas tungsten arc welding (GTAW) torch with a gas hood was used in the experiments; the schematic diagram is shown in Fig. 1. Nitrogen was added into the shielding gas through the gas hood. The pure Ar used to generate the arc and protect the pool and electrode from oxidation is at the inner layer, and the N_2 is at the outer layer. In this investigation, the power source was

Table 2 Chemical compositions of 443 ferritic stainless steel (wt%)

Alloy element	C	Cr	Si	Cu	P	S	N	Mn	Ti	Fe
Content	<0.01	21	0.3	0.4	≤0.02	≤0.002	0.012	0.1	0.2	Bal.

Table 3 Properties of 443 ferritic stainless steel

$R_{P0.2}$ (MPa)	Rm (MPa)	A (%)	$HV_{0.1}$
330	480	33	153

Times WS-250 with direct current electrode negative polarity. Four experimental conditions were employed in this study. The welding parameters are listed in Table 1.

The base material used for this study was 443 ferrite stainless steel sheets, with the dimensions of 200 × 60 × 3 mm. Its chemical compositions and mechanical properties are listed in Table 2 and 3 respectively. Before welding, the sheets were polished by sandpaper to expose metallic luster and cleaned by acetone. After welding, the welds were etched in $FeCl_3$ liquid with HCl, HNO_3, and water for about 15 s. The microstructure was analyzed by optical microscopy to study the effect of nitrogen on the microstructures of 443 ferritic stainless steel welds. Vickers hardness was measured under a load of 300 N. In order to investigate the effect of nitrogen on the impact toughness of 443 ferritic stainless steel welds, specimens selected from conditions 1, 2, and 4 which are welded by the same welding conditions except for the contents of nitrogen in the shielded gas were tested for the Charpy impact testing at 20 °C. Two samples, with the dimensions of 50 × 10 × 3 mm, different in the position of v-notch which one was at the center of weld bead and another was at HAZ from conditions 1, 2, and 4 separately were impacted. The feature of the specimen's impact fracture was analyzed in scanning electron microscope (SEM) and energy-dispersive spectrometer (EDS).

3 Results

3.1 Macrostructure of the joints

The cross sections of the welds tested in conditions 1, 2, 3, and 4 are presented in Fig. 2a–d, respectively. The depth/width (*D*/*W*) ratios and the width of HAZ of the welds in various conditions are presented in Fig. 3. By comparing the conditions 1 and 2, the *D*/*W* ratio of weld protected by simple double-layer gas was increased compared with that protected by pure argon. *D*/*W* ratio decreased with the increase of heat input by comparing the conditions 2 and 3. The minimal *D*/*W* ratio appeared in condition 4 which is protected by mixed double-layer gas. The width of HAZ in the weld joint in condition 2 was less than that in conditions 1 and 3 while more than that in condition 4 which was the minimum. The width of HAZ in condition 3 was the maximum, because its heat input was the maximum.

3.2 Microstructure of the joints

The microstructures in the center of the welds in conditions 1, 2, 3, and 4 are presented in Fig. 4a–d, respectively. The microstructures in HAZ in conditions 1, 2, 3, and 4 are presented in Fig. 5a–d, respectively. In conditions 2 and 3, the microstructures of the welds were made up of equiaxed grains, which are located in the weld center, and columnar grains around the weld center. The microstructure was composed of columnar grains and some amounts of equiaxed grains located between columnar grains in the weld of condition 4. While in condition 1, equiaxed grains could not be observed and all of the weld area was columnar grains. The average sizes of the equiaxed grains in conditions 2 and 3 were 47.7 and 55.6 μm, respectively. Additionally, the equiaxed grains were accounted for 23.11 and 19.56 % of the entire weld beads in conditions 2 and 3, respectively.

Hence, the average sizes of columnar in conditions 2, 3, and 4 were almost the same but smaller than that in conditions 1. The average size of equiaxed grains in condition 2 was smaller than that in condition 3. It was due to that the heat input in condition 3 was more than that in condition 2. The molten pool cooled more slowly, and the cooling time was prolonged. Therefore, the grains grew coarser in condition 3. While the proportion of equiaxed grains in the weld in condition 3 was smaller than that in condition 2, it is because that the heat input of the weld in condition 3 was greater. The greater heat input reduced the undercooling degree of the weld pool. Therefore, the quantity of the crystal nucleus had been reduced in condition 3 compared with that under the condition of 2.

Otherwise, there were some equiaxed crystals distributed among the broken columnar crystals between the equiaxed crystal zone and columnar crystal zone in conditions 2 and

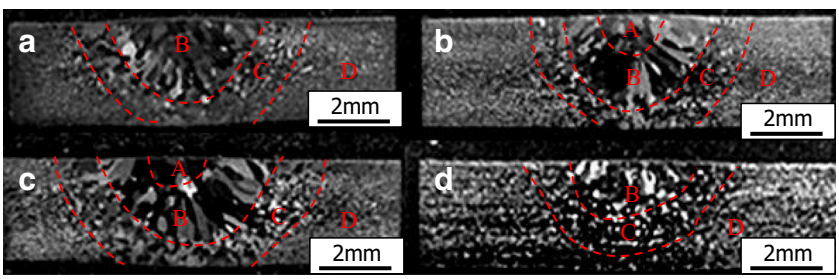

Fig. 2 Cross sections of the welds: *A* equiaxed zone, *B* columnar zone, *C* HAZ, and *D* base metal. **a** Cross section in condition 1. **b** Cross section in condition 2. **c** Cross section in condition 3. **d** Cross section in condition 4

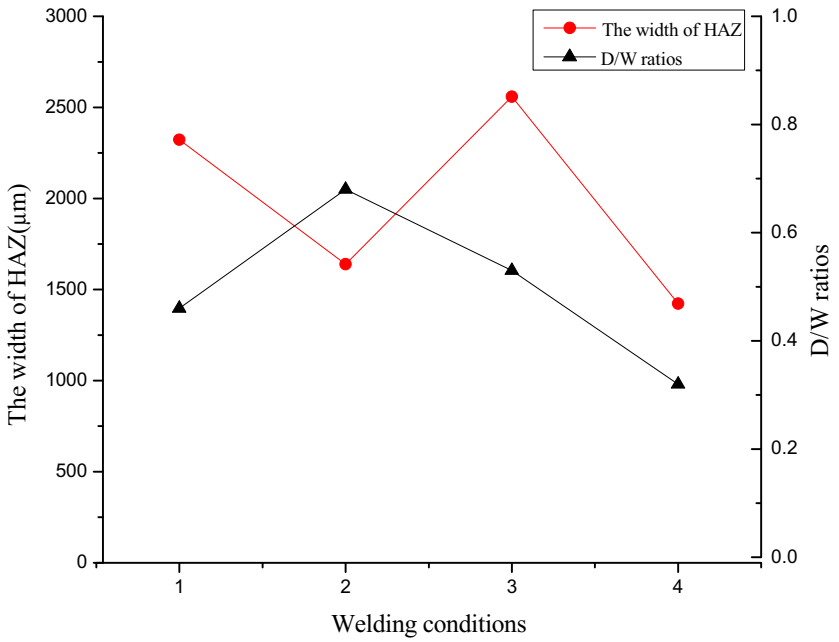

Fig. 3 Width of HAZ and *D*/*W* ratio of weld in various conditions

3. It was because that when the columnar crystals were not completely solidified, there were certain amounts of liquid metal between columnar crystals. Some crystal nucleus ran into the liquid metal between columnar crystals. With the effect of stirring and breaking by electric arc on columnar grains, some broken columnar grains and some equiaxed grains have been retained in front of the columnar crystal zone, presented in Fig. 6.

The average sizes of the grains in the HAZ and the columnar grains in the welds in conditions 1, 2, 3, and 4 are shown in Fig. 7. It revealed that the average sizes of the grains in the HAZ and the columnar grains in the welds in condition 2 were smaller than those in conditions 1 and 3. In condition 4, the average size of columnar grains was smallest and that of grains in the HAZ was almost the same as condition 2.

3.3 Hardness

The Vickers hardness distribution across the weld joints was measured at 0.5-mm intervals in the lateral direction. The

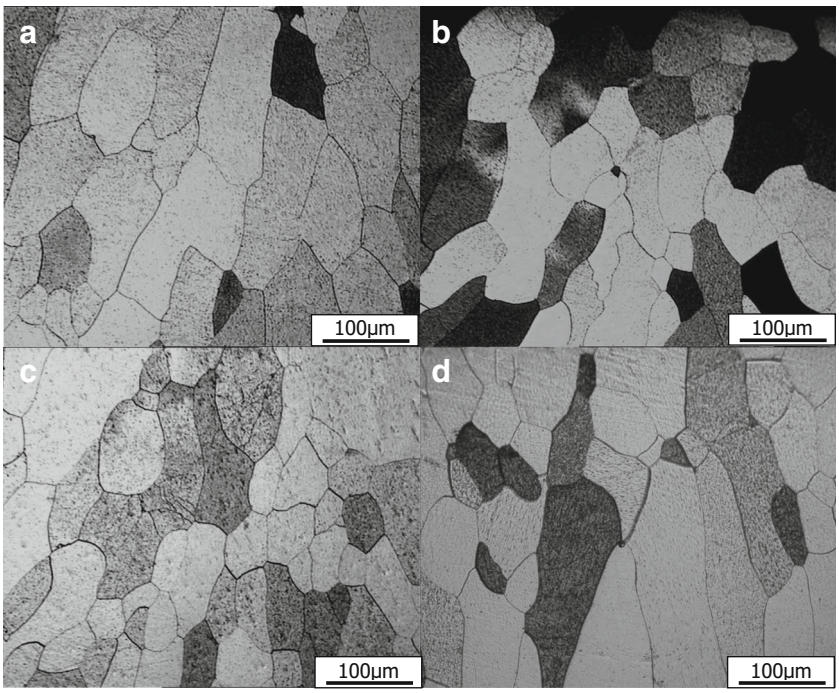

Fig. 4 Microstructure of the central welds **a** in condition 1, **b** in condition 2, **c** in condition 3, and **d** in condition 4

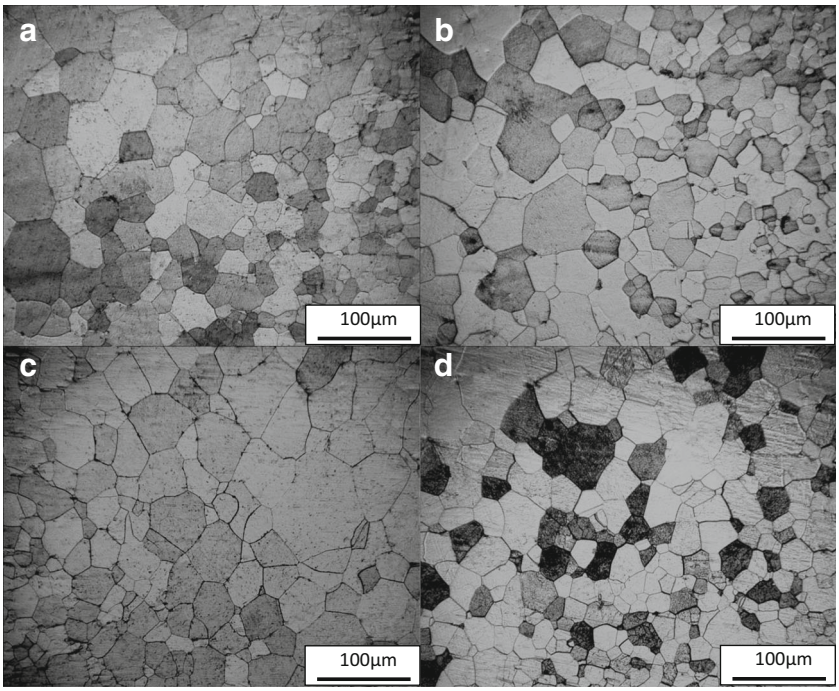

Fig. 5 Microstructure of the HAZ **a** in condition 1, **b** in condition 2, **c** in condition 3, and **d** in condition 4

results in different welding conditions are presented in Fig. 8. It was significant to note that the central hardness of the welds in conditions 2 and 3 was higher than that of in conditions 1 and 4. The largest values of hardness at the center of the welds in conditions 2 and 3 were 211.9HV and 229HV, respectively. While in conditions 1 and 4, the hardness values were 172.4HV and 165.5HV, respectively. Generally speaking, the smaller the grain size, the greater the hardness. The obviously higher hardness at the center of the welds protected by simple double-layer gas could be explained by the appearance of fine equiaxed crystals in this zone, while the hardness at the center of welds in conditions 1 and 4 was lower because the crystals in the zone were coarse columnar grains. The hardness of HAZ in condition 4 was the largest.

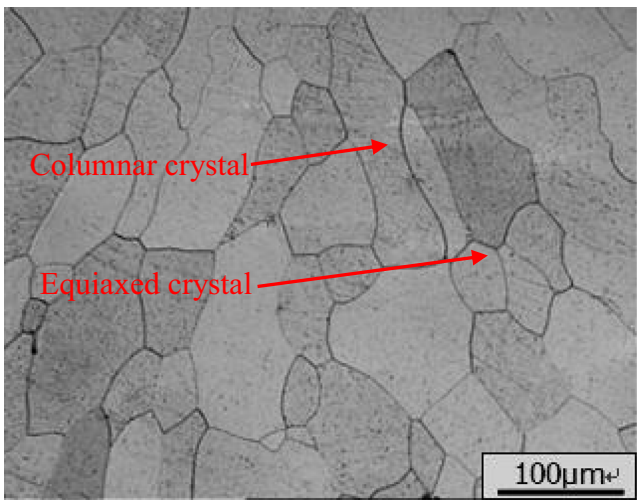

Fig. 6 Equiaxed crystals between the columnar crystals

3.4 The Charpy impact and fractograph

The results of Charpy impact testing are shown in Table 4. It has shown that the impact toughness values both of weld bead and HAZ in condition 2 were larger than those in condition 1. Therefore, the impact toughness of the weld bead and HAZ in condition 2 protected by simple double-layer gas was better than that in condition 1 which is protected by pure Ar. Because the weld in condition 2 contained equiaxed zone and columnar grain zone, the average size of columnar grains was the smallest of all. However, the all weld was composed of columnar grains whose average size of grains was the largest in condition 1. The impact energy of the weld joint in condition 4 was between that in conditions 2 and 1 no matter in weld bead or HAZ. Because the weld bead in condition 4 was consisted of columnar grains with equiaxed grains mixed, it had a middle size of grains. Similarly, the grains of HAZ in condition 2 were the finest, while that in condition 1 was the coarsest and that in condition 4 was in the middle. Impact energy in condition 4 was larger than that in condition 1 but smaller than that in condition 2.

The fractures of the impacted samples in conditions 1 and 2 were analyzed by SEM and EDS. It emerged equal-axis ductile voids in the SEM fractographs in condition 2, present in Fig. 9. As the v-notch chiseled at the center of weld bead, some particles could be found in the ductile voids, as shown in Fig. 9a. The results of EDS analysis of particle 1 and particle 2 have shown that the contents of nitrogen were 12.9 and 15.2 %, respectively, as shown in

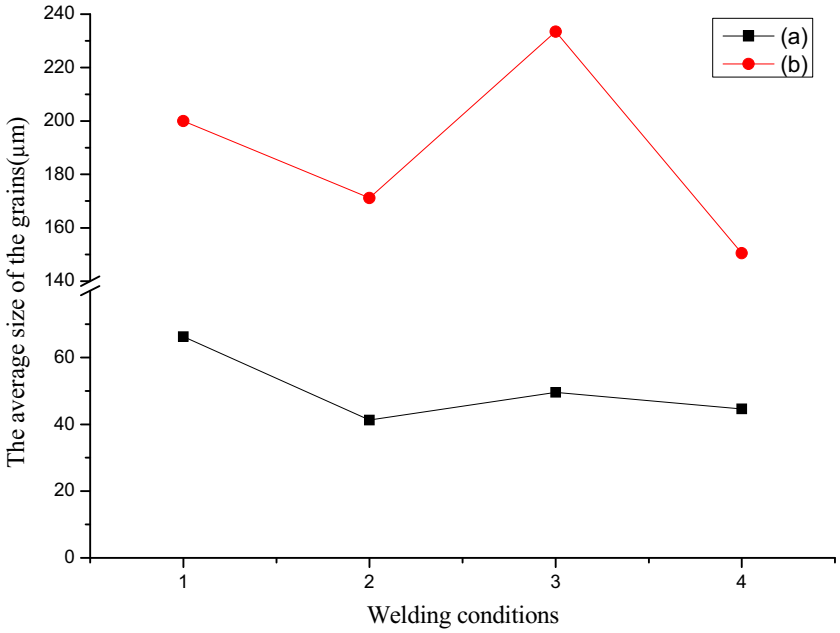

Fig. 7 *a* The average size of grains in HAZ in various conditions. *b* The average size of columnar grains in welds in various conditions

Fig. 10, while there were almost no particles in the ductile voids in HAZ. But, both of the two specimens were mainly brittle fracture in condition 2. There were cleavage steps in the SEM fractographs in condition 1, no matter the v-notch chiseled at the center of weld bead or HAZ, presented in Fig. 11. In addition, there were tongue pattern and secondary crack in condition 1 when the v-notch chiseled at HAZ, as shown in Fig. 11b. It could get that the specimens in conditions 1 and 2 were brittle fracture from the results of Charpy impact experiment. It was because that the crystals in the joints were coarser compared with base metal crystals.

4 Discussions

In this study, the effect of nitrogen on the *D*/*W* ratio of the weld might be explained by that N_2 had the ability to change the surface tension temperature coefficient of the molten pool. Similar phenomenon was reported by Shanping Lu et al. [20] about the effect of oxygen on the Marangoni convection in the molten pool. The welds with N_2 in the shielding gas cooled more rapidly than that without N_2 because the thermal conductivity of nitrogen is larger than argon. Thus, it increased the cooling rate of the welds and reduced both the size of grains and the width of HAZ. It resulted to a narrower HAZ

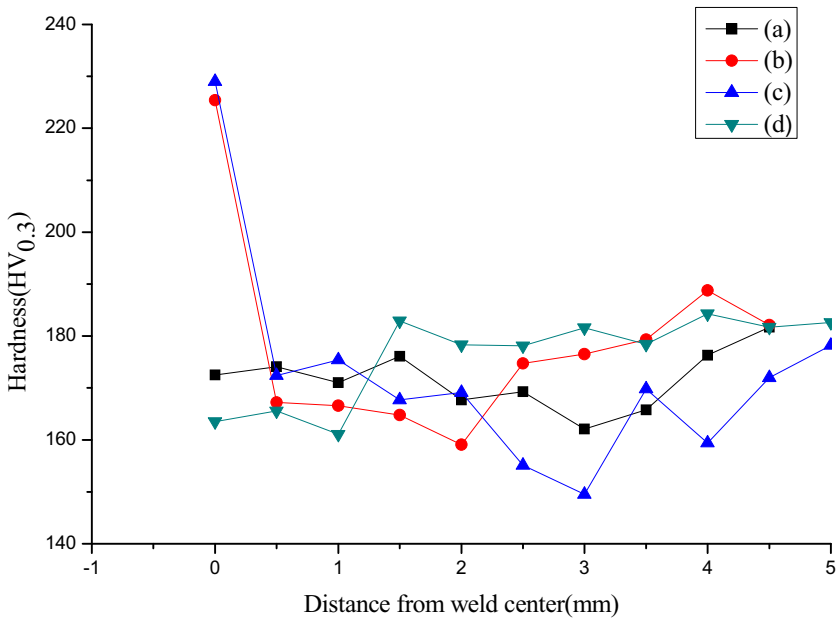

Fig. 8 Vickers hardness distributions of the weld *a* in condition 1, *b* in condition 2, *c* in condition 3, and *d* in condition 4

Table 4 Result of Charpy impact testing in conditions 1, 2, and 4 at 20 °C

	Impact energy of weld bead (J)	Impact energy of HAZ (J)
Condition 1	2	8
Condition 2	7.8	20
Condition 4	5	15

and finer grains in HAZ when the N_2 was added in the shielded gas. However, heat input had a great influence on them. The width and the average grain size of HAZ were the maximal of all.

In general, the weld grains condensed on the edge of the heat-affected zone of the base metal in the initial stage of the molten pool solidification, and then, they gradually extended to the weld pool center to form the columnar grains. The solidification model in condition 1 in this study just was like this. But, with the N_2 dissolved in the molten pool, it might increase the undercooling degree and reduce the temperature gradient of the molten pool during welding process, as shown in Fig. 12. Therefore, the growth rate of the columnar crystal decreased with the decrease of temperature gradient. Meanwhile, some nitrogen-titanium (TiN) particles, presented in Figs. 9 and 11, were precipitated in the molten pool with the molten pool cooled down. In the late stage of the molten pool solidification, some of the TiN particles acted as crystal nucleus and grew into equiaxed grains because the heat dissipation had lost directions and the grains growth rate was the same along each direction. Finally, the columnar grains and equiaxed grains grew up at the same time until meeting to stop. It eventually formed equiaxed grains in the weld center. The appearance of the equiaxed crystals was an obstacle to the growth of columnar crystals. Hence, the weld microstructure was composed of equiaxed crystal zone and columnar crystal zone. However, the columnar crystals in the weld without N_2 would stretch into the weld center with a faster rate. So, the weld was made up of whole columnar crystals. The molten pool became shallower and wider by the addition of excess nitrogen, in condition 4, which may lead a negative surface tension temperature coefficient. Hence, the molten pool cooled faster and the columnar grains grew faster and filled the entire weld soon. Therefore, there was lack of enough time for the equiaxed crystal nucleus to precipitate or grow. As a result, there was a small amount of equiaxed grains between the columnar grains (Fig. 4d).

Generally speaking, the smaller the grain size, the greater the hardness. The hardness in the welds could be increased by the function of grain refinement of N_2. In the HAZ, solid dissolution of N atoms might produce a distorted lattice of Fe matrix which results in an increase in the hardness of the steel [18, 21]. Both in weld and in HAZ, with the finer grains, the amounts of grain boundaries were more. Hence, the crack propagation resistance was increased and it needed greater energy for crack to propagate. Therefore, impact toughness was improved.

5 Conclusions

In this study, a double-layer gas-shielded welding method was implemented for the welding of 443 ferrite stainless steel, the inner gas was Ar or Ar-5 %N_2 and the outer was N_2. The main conclusions of this study may be summarized as follows:

1. In the center of the welds protected by N_2 and Ar, it formed equiaxed grains while there were all columnar grains in the weld protected by pure Ar. In the welding, when the protected gas was simple double-layer gas but the currents were 80 and 100 A, the areas of equiaxed grains accounted for 23.11 and 19.56 % of the entire weld metal, respectively.
2. The *D*/*W* ratio of the weld has been increased by the addition of N_2 at the outer layer of the pure Ar as shielding gas.

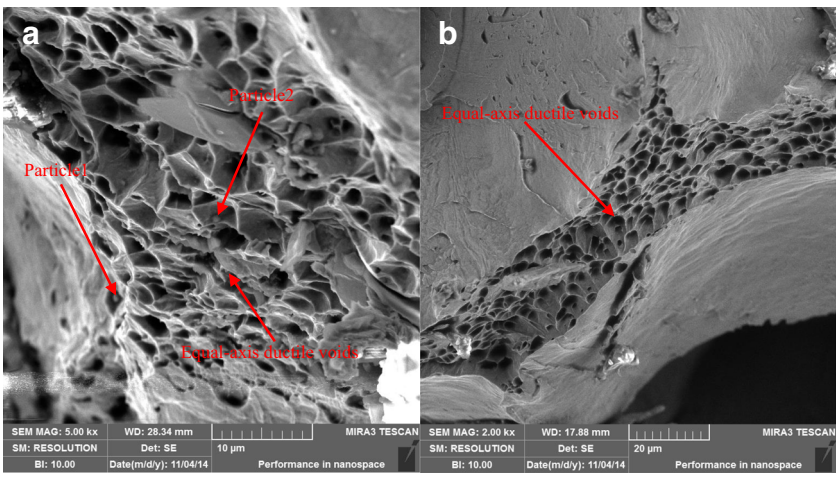

Fig. 9 SEM fractographs of condition 2: **a** v-notch chiseled at the center of weld bead and **b** v-notch chiseled at HAZ

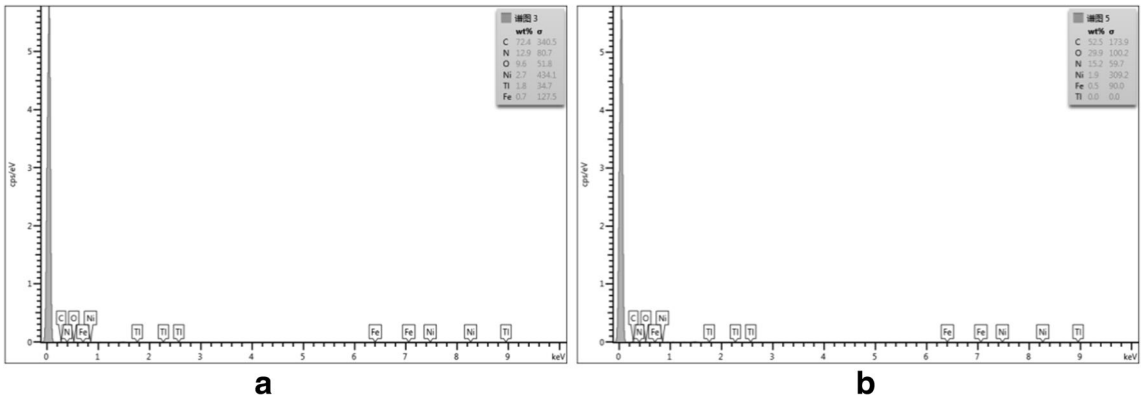

Fig. 10 The EDS results: **a** the results of particle 1 and **b** the results of particle 2

The D/W ratio of the weld with N_2 at the outer layer of the pure Ar as shielding gas could be achieved 0.68 while it was 0.46 with pure Ar as shielding gas. It was increased by 47.8 %.

3. The impact energy of the weld bead with N_2 added at the outer layer of the pure Ar as shielding gas, compared with no N_2, was improved from 2.0 to 7.8 J. The impact energy of the

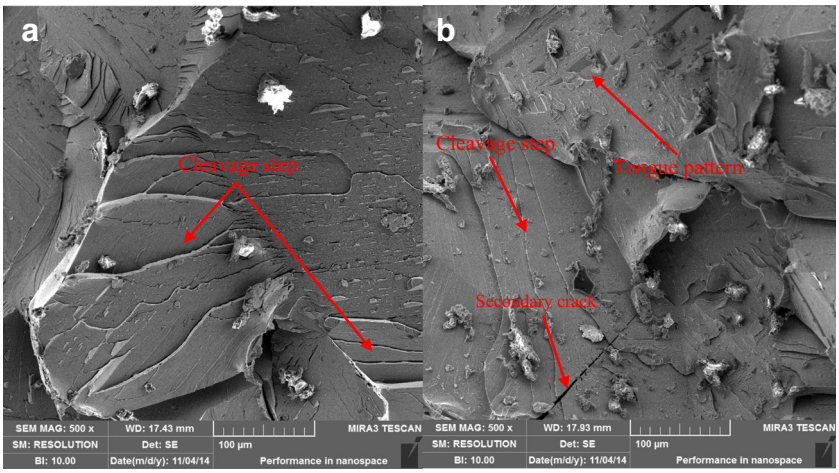

Fig. 11 SEM fractographs of condition 1: **a** v-notch chiseled at the center of weld bead and **b** v-notch chiseled at HAZ

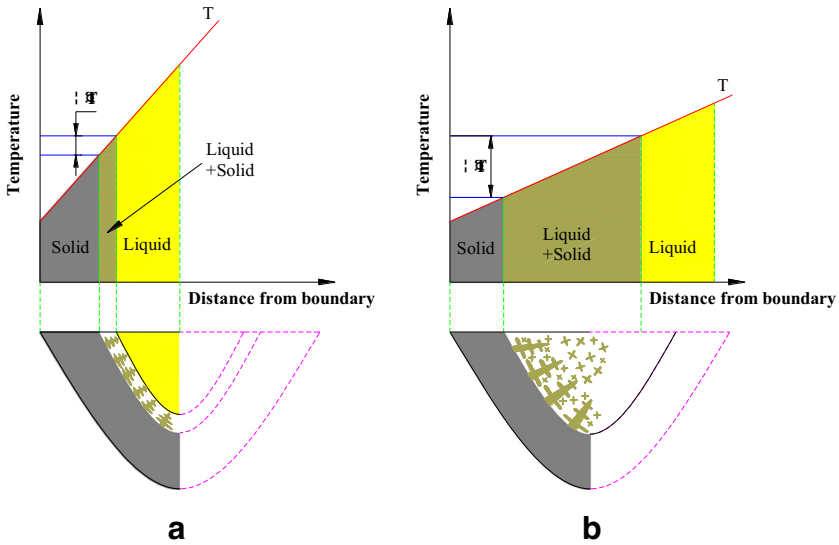

Fig. 12 Schematic diagram of weld pool solidification mode in different undercooling degrees and temperature gradients **a** shielded by pure Ar and **b** shielded by simple double-layer gas

HAZ with N_2 added at the outer layer of the pure Ar as shielding gas, compared with no N_2, was improved from 15.0 to 20.0 J.

Acknowledgments This work was supported by the National Natural Science Foundation of China under Grant (No. 51305291) and Natural Science Foundation of Shanxi Province (No. 201302121-1).

References

1. Mallaiah G, Kumar A, Ravinder Reddy P, Madhusudhan G (2012) Influence of grain refining elements on mechanical properties of AISI 430 ferritic stainless steel weldments—Taguchi approach[J]. Mater Des 36:443–450
2. Amuda MOH, Mridha S (2012) Comparative evaluation of grain refinement in AISI 430 FSS welds by elemental metal powder addition and cryogenic cooling[J]. Mater Des 35:609–618
3. Zhang H, Hu SS, Shen JQ, Ma L, Yin FL (2015) Microstructures and mechanical properties of 30Cr-4Mo ferritic stainless steel joints produced by double-pulsed gas metal arc welding. Int J Adv Manuf Technol 80:1975–1983
4. Tae JP, Jong PK, Sang HU, In SW, Jong SL, Chung YK (2011) Effect of Al–Si coating layer on the penetration and microstructures of ferritic stainless steel, 409L GTA welds[J]. J Mater Process Technol 211(3):415–423
5. Amuda MOH, Mridha S (2013) Grain refinement and hardness distribution in cryogenically cooled ferritic stainless steel welds[J]. Mater Des 47:365–371
6. Watanabe T, Nakamura H, Ei K (1989) Grain refinement by TIG welding with electromagnetic stirring—a study of solidification control of austenitic stainless steel weld metal[J]. Weld Int 3(4): 312–317
7. Liu Z, Su M, Su Y (2009) Influence of magnetic field on microstructure and properties of stainless steel welding joint [J]. J Shenyang Univ Technol 6:014
8. Watanabe T, Shiroki M, Yanagisawa A, Sasaki T (2010) Improvement of mechanical properties of ferritic stainless steel weld metal by ultrasonic vibration[J]. J Mater Process Technol 210(12):1646–1651
9. Li DJ, Lu SP, Li DZ, Li YY (2010) Mechanisms increasing welding efficiency during new development of double shielded TIG process[J]. Sci Technol Weld Joining 15(6):528–533
10. Lakshminarayanan AK, Balasubramanian V (2010) An assessment of microstructure, hardness, tensile and impact strength of friction stir welded ferritic stainless steel joints[J]. Mater Des 31(10):4592–4600
11. Lakshminarayanan AK, Balasubramanian V (2012) Evaluation of microstructure and mechanical properties of laser beam welded AISI 409 M grade ferritic stainless steel[J]. J Iron Steel Res Int 19(1):72–78
12. Sprengard BA (2011) Effect of nitrogen concentration in shielding gas on microstructure and mechanical properties of ATI 2003® Lean Duplex Stainless Steel Autogenous Plasma Arc Welding[D]. University of Cincinnati
13. Keskitalo M, Mäntyjärvi K, Sundqvist J, Powell J, Kaplan AFH (2015) Laser welding of duplex stainless steel with nitrogen as shielding gas[J]. J Mater Process Technol 216:381–384
14. Pan DZ (2012) Physical simulation of variations in nitrogen content in laser welds of 21-6-9 austenitic stainless steel alloys. The Ohio State University
15. Villafuerte JC, Pardo E, Kerr HW (1990) The effect of alloy composition and welding conditions on columnar-equiaxed transitions in ferritic stainless steel gas-tungsten arc welds[J]. Metall Trans A 21(7):2009–2019
16. Villaret V, Deschaux-Beaume F, Bordreuil C, Rouquette S, Chovet C (2013) Influence of filler wire composition on weld microstructures of a 444 ferritic stainless steel grade[J]. J Mater Process Technol 213(9):1538–1547
17. Villafuerte JC, Kerr HW, David SA (1995) Mechanisms of equiaxed grain formation in ferritic stainless steel gas tungsten arc welds[J]. Mater Sci Eng A 194(2):187–191
18. Akhlaghi M, Steiner T, Meka SR, Leineweber A, Mittemeijer EJ (2015) Lattice-parameter change induced by accommodation of precipitate/matrix misfit; misfitting nitrides in ferrite[J]. Acta Mater 98:254–262
19. Sathiya P, Jaleel AMY (2011) Influence of shielding gas mixtures on bead profile and microstructural characteristics of super austenitic stainless steel weldments by laser welding. J Mater Process Technol 54:525–535
20. Lu S, Fujii H, Nogi K (2004) Marangoni convection and weld shape variations in Ar–O_2 and Ar–CO_2 shielded GTA welding[J]. Mater Sci Eng A 380(1):290–297
21. Li JY, Chen YL, Huo JH (2015) Mechanism of improvement on strength and toughness of H13 die steel by nitrogen[J]. Materials Science and Engineering: A